Available online at www.sciencedirect.com

ScienceDirect

J. Differential Equations 268 (2019) 301–317

Journal of Differential Equations

www.elsevier.com/locate/jde

Results from a differential equation model for cell motion with random switching show that the model cell velocity is asymptotically independent of force

J.C. Dallon, Emily J. Evans *, Christopher P. Grant, W.V. Smith

Department of Mathematics, Brigham Young University, Provo, UT 84602, USA

Received 25 December 2016; revised 9 November 2018; accepted 15 August 2019
Available online 27 August 2019

Abstract

Numerical simulations suggest that average velocity of a biological cell depends largely on attachment dynamics and less on the forces exerted by the cell. We determine the relationship between two models of cell motion, one based on finite spring constants modeling attachment properties (a randomly switched differential equation) and a limiting case (a centroid model-a generalized random walk) where spring constants are infinite. We prove the main result of this paper, the Expected Velocity Relationship theorem. This result shows that the expected value of the difference between cell locations in the differential equation model at the initial time and at some elapsed time is proportional to the elapsed time. We also show that the relationship is time invariant. Numerical results show the model is consistent with experimental data.

Keywords: Randomly switched equations; Markov chain; Expectation; Discrete process; Continuous process

1. Introduction

Numerical simulations and experimental measurements suggest that the speed at which a biological cell moves is far more dependent on the binding dynamics of the adhesion sites the cell creates on substrate materials (and other cells) than on the magnitude of force it exerts on

* Corresponding author.
E-mail address: ejevans@mathematics.byu.edu (E.J. Evans).

https://doi.org/10.1016/j.jde.2019.08.019

those surroundings. Those dynamics are the key to predicting cell speed. In [4] we introduced an ordinary differential equation model for cell motion relative to a probability distribution η on some outcome space Ω,

$$\mu \mathbf{x}' = \sum_{i=1}^{n} -\alpha_i (\mathbf{x} - \mathbf{u}_i)\psi_i(t),$$

where $\mathbf{x}$ is a vector process defining the cell center in "cell space," and the α_i are Hookian (spring) constants that model forces exerted by adhesion sites located at $\mathbf{u}_i$ (also a vector process). This model incorporates the nature of adhesion sites using the randomly switched functions ψ_i which take the values 0 or 1 depending on whether the ith site is detached or attached to the substrate.

In [2] we considered a limiting case of this differential equation model—as the spring constants α_i increase without bound—which results in a discrete-time centroid model that tracks the centroid of the attachments sites of the cell after each site attachment or detachment event. The discrete-time centroid model is a Markov chain and is generated by a transition kernel. In that paper we also introduced the expected average velocity relationship conjecture (EVR conjecture) which states that, in the limiting case, the expected average velocity of the cell is independent of the cell forces and dependent on the binding dynamics for the differential equation model.

In [1], we extended our results from the discrete-time centroid model to a continuous-time centroid model which tracks the location of the centroid by time instead of event. We showed that the continuous-time centroid model is in fact a pure jump-type continuous-time Markov process generated by a rate kernel and gave a formula for the velocity of the expected value of the centroid.

In this paper we state and prove the EVR conjecture for the differential equation model. The EVR conjecture is reasonable because of the saltatory nature of cell adhesion. Effectively motion is lost when speeds and velocities are averaged over short periods of time. That average is largely independent of cell force and highly dependent on the on-off nature of adhesion. This is the EVR conjecture which is stated and proved in Section 4. We begin in Section 2 with a review of the differential equation model. Then in Section 3 we review the results of the continuous-time centroid model and its relationship to the differential equation model. The proof of the EVR theorem is based on a series of lemmas given in Section 4.2 and is completed in Section 4.3. We conclude with discussions of numerical techniques, the biological relevance of the results, and future mathematical challenges.

2. Differential equation model

The cell is modeled as a nucleus and multiple interaction sites which exert forces on the nucleus as illustrated in Fig. 1. These interaction sites are known as integrin based adhesion sites (I-sites) [6,7,10]. I-sites attach to an external substrate and once attached remain fixed to that substrate location for a period of time. The duration of the attachment is determined by a given probability distribution. The same is true for the time the I-site remains unattached, although the distributions need not be the same. The differential equation model assumes the I-sites exert forces on the nucleus according to Hooke's law; that is, the force is proportional to distance. Thus it is as if the I-sites are attached to the cell center with springs which have a rest length assumed to be zero. Moreover there is a drag force (proportional to the velocity) on the cell nucleus which is modeled assuming the center (nucleus) is a sphere in a liquid with low Reynolds number. The

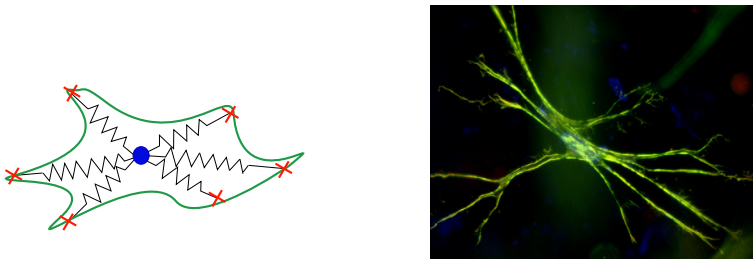

Fig. 1. The left panel depicts the way a cell is modeled mathematically. The right panel is a fibroblast in a collagen lattice. Note the similarity of the model formation with the typical spindal morphology of a fibroblast in a three dimensional lattice. The cell is a center location (nucleus) with attached springs. The other end of the springs are attached to sites which can interact with the extracellular matrix (membrane bound adhesion sites) depicted by "x".

cell center $\mathbf{x}$ is considered to be a point in $\mathbb{R}^N$. Likewise the location of each I-site $\mathbf{u}_i$ is a point in $\mathbb{R}^N$, where i ranges from 1 to n. The small scale allows the assumption of low Reynolds number and therefore any acceleration term may be neglected [3]. The equation defining the cell center as given in the introduction is

$$\mu \mathbf{x}' = \sum_{i=1}^{n} -\alpha_i (\mathbf{x} - \mathbf{u}_i)\psi_i(t). \tag{1}$$

Here μ is the drag coefficient for the nucleus. The equation for the location of the ith I-site is

$$\mathbf{u}_i(t) = \lim_{y \nearrow a_{p,i}} \mathbf{x}(y) + \mathbf{b}^{p,i} \text{ for } a_{p,i} \le t < a_{p+1,i}.$$

For each i the sequence $\{a_{p,i}\}$ of random variables are the times when ψ_i makes the transition from 0 to 1, and $\{d_{p,i}\}$ is the sequence of random variables of the times when ψ_i makes the transition from 1 to 0. Of course, the two sequences are not independent since $a_{p,i} < d_{p^*,i} < a_{p+1,i}$ where $p^* = p$ if the initial state starts with the ith I-site detached and $p^* = p + 1$ if it starts out attached. The vectors $\mathbf{b}^{p,i}$ are independent, identically distributed random vectors with respect to the assumed distribution η and $\mathbf{b}$ has mean $\overline{\mathbf{b}}$. Although the equations of motion are independent of the location of the I-site when it is detached, for convenience we assume the location does not change until it reattaches.

3. Centroid model

The differential equation model may be approximated heuristically by a problem that tracks the centroid of the attachment sites (or the center if no attachments exist). This new problem is motivated by informally considering the limit of the differential equation model as the spring constants become very large. In this limit, one expects the smooth motion of the cell nucleus to disappear and the centroid to jump from position to position. Let $\mathbf{c}$ denote the centroid. It is defined by

$$0 = \sum_{i=1}^{n} \alpha_i (\mathbf{c} - \mathbf{u}_i)\psi_i$$

which may be written as

$$\mathbf{c} = \sum_{i=1}^{n} \frac{\alpha_i}{\sum_{j=1}^{n} \alpha_j \psi_j} \mathbf{u}_i \psi_i.$$

3.1. Notational conventions

Let $\Psi = (\psi_1, \psi_2, \cdots, \psi_n)$, $|\Psi| = \sum_{i=1}^{n} \psi_i$, $\mathbf{u} = (\mathbf{u}_1, \cdots, \mathbf{u}_n)$ and ω be the outcome variable. The subscript Z indicates variables from the continuous-time centroid model and the subscript DE indicates variables from the differential equation model. The variable $\mathbf{c}$ is used to denote the location of the centroid for either model and the variable $\mathbf{x}$ denotes the location of the cell center in either model (as indicated by the subscript). We define the cell center in the centroid model to be the centroid, that is, $\mathbf{x}_Z = \mathbf{c}_Z$. Let

$$\mathbf{y}_{DE} = (\mathbf{x}_{DE}, \mathbf{c}_{DE}, \mathbf{u}_{DE}) : [0, \infty) \to \mathbb{R}^N \times \mathbb{R}^N \times (\mathbb{R}^N)^n$$

and

$$\mathbf{y}_Z = (\mathbf{x}_Z, \mathbf{c}_Z, \mathbf{u}_Z) : [0, \infty) \to \mathbb{R}^N \times \mathbb{R}^N \times (\mathbb{R}^N)^n$$

be, respectively, the differential equation solution and the continuous-time centroid solution corresponding to the same initial conditions and same outcome ω. We assume that these solutions (and the accompanying $\Psi(t)$) are right-continuous and have left-hand limits, with the left-hand limit at time t being represented by evaluation at t^-. Let $\|\cdot\|$ be the norm on $\mathbb{R}^N \times \mathbb{R}^N \times (\mathbb{R}^N)^n$ defined by

$$\|\mathbf{y}\| = \|(\mathbf{x}, \mathbf{c}, (\mathbf{u}_1, \mathbf{u}_2, \ldots, \mathbf{u}_n))\| = \max\{|\mathbf{x}|, |\mathbf{c}|, |\mathbf{u}_1|, |\mathbf{u}_2|, \ldots, |\mathbf{u}_n|\},$$

where $|\cdot|$ is the Euclidean norm on $\mathbb{R}^N$.

3.2. Continuity properties of the expectation

We now review important results for the continuous-time centroid model introduced in [1]. Assume that the wait time for an attached I-site to detach ($a_{p+1,i} - d_{p^*,i}$) is exponentially distributed with parameter θ_d (so that the mean time to detach is $1/\theta_d$), and the wait time for a detached I-site to attach ($d_{p^*,i} - a_{p,i}$) is exponentially distributed with parameter θ_a. Each of these wait times is assumed to be independent of the other wait times and of the model's other random parameters. When an I-site attaches, it does so at a point whose displacement from the centroid of attached I-sites is a bounded random quantity with distribution η. In [1], the following was shown: for arbitrary initial conditions there is a pure-jump type Markov process that obeys this evolution law. There is a corresponding pure-jump type Markov process with finite state space $\{0, 1, \ldots, n\}$ that tracks only how many I-sites are attached ($|\Psi|$). Let's call the first process the "full process" and the second process the "projected process". The projected process has a unique invariant distribution σ, and regardless of the initial distribution of the projected process, the distribution of the process at time t will converge to σ as $t \to \infty$. If the full process is equipped with an initial distribution that is compatible with σ and such that the locations of

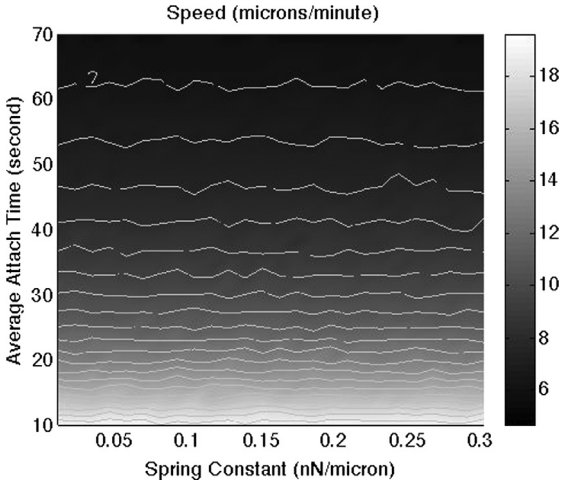

Fig. 2. The speed of a single cell is plotted against the mean attach time and strength of the cell. The cell speed is remarkably constant with respect to the strength of the cell. The contour lines are plotted over the shading. The plot shows the average of 50 random runs for each data point. The mean detach time is 25 seconds with a "continuous Poisson distribution" and the attach time is taken from a continuous Poisson distribution. The continuous Poisson distribution is a distribution which when rounded to the integers is a Poisson distribution [9]. The speed was calculated in the simulations by averaging over a 60 second time interval. The smallest value for α plotted is 0.01.

the I-sites and of the centroid of attached I-sites all have well-defined expected values, then the derivative with respect to t of the expected location of the centroid of attached I-sites at time t is

$$\frac{\partial}{\partial t}\mathbb{E}(\mathbf{c}(t)) = \frac{\overline{\boldsymbol{b}}\theta_d}{(\theta_d+\theta_a)^n}\left((\theta_d+\theta_a)^n - \theta_d^n\right). \tag{2}$$

4. The expected average velocity relationship theorem

4.1. EVR theorem

Numerical simulations suggested and helped to formulate the EVR. Assume that $\alpha_i = \alpha$ for all i. Simulations of a single cell indicate that the speed of the cell is essentially independent of the spring constant α (see Fig. 2) for a wide range of relevant values. Of course, when $\alpha = 0$, the cell does not move and for values near zero the speed will approach zero. A precise mathematical formulation of this phenomenon is as follows.

Theorem 4.1 *(EVR Theorem). Assume the initial configuration for* (1) *is randomly distributed in a way that is compatible with the steady-state distribution* σ. *Moreover assume* $\alpha_i = \alpha$ *for all* i *and that* $\mathbf{x}_{DE}(0) = \mathbf{x}_Z(0)$ *(corresponding to the equilibrium position of the deterministic problem). For any fixed time* $t > 0$,

$$\lim_{\frac{\alpha}{\mu}\to\infty} \mathbb{E}[\mathbf{x}(t) - \mathbf{x}(0)] = \boldsymbol{\zeta} t,$$

where $\boldsymbol{\zeta}$ is independent of α but depends on the number (n) of I-sites, their mean time to attach ($1/\theta_a$), their mean time to detach ($1/\theta_d$), and the mean ($\bar{\boldsymbol{b}}$) of their perturbations when a new attachment occurs. More specifically,

$$\boldsymbol{\zeta} = \frac{\bar{\boldsymbol{b}}\theta_d}{(\theta_d+\theta_a)^n}\left((\theta_d+\theta_a)^n - \theta_d^n\right).$$

4.2. Preliminary lemmas

Prior to the proof of the EVR theorem we need two preliminary lemmas. The first lemma bounds the distance between $\mathbf{y}_Z$ and $\mathbf{y}_{DE}$ and thus the distance between $\mathbf{x}_Z$ and $\mathbf{x}_{DE}$. More precisely, given the distance between $\mathbf{y}_Z$ and $\mathbf{y}_{DE}$ at the instant before a binding event occurs we find a bound on the distance between $\mathbf{y}_Z$ and $\mathbf{y}_{DE}$ at the instant before the next binding event occurs.

Lemma 4.2. *Assume that an attachment/detachment event occurs at time $t_1 > 0$, that $t_2 > t_1$, and that no attachment/detachment events occur on (t_1, t_2). Define*

$$M := \|\mathbf{y}_{DE}(t_1^-)\|,$$

and let B be such that $\eta(\mathcal{B}(0,B)) = 1$. Then

$$\|\mathbf{y}_{DE}(t_2^-) - \mathbf{y}_Z(t_2^-)\| \le \|\mathbf{y}_{DE}(t_1^-) - \mathbf{y}_Z(t_1^-)\| + (2M+B)\exp\left(-\frac{(t_2-t_1)\min_i \alpha_i}{\mu}\right) \quad a.s.$$

Proof. Almost surely for small $\delta > 0$, changes (if any) in $\mathbf{u}_{DE}$, $\mathbf{u}_Z$, $\mathbf{c}_{DE}$, $\mathbf{c}_Z$, and $\mathbf{x}_Z$ on $(t_1 - \delta, t_2)$ occur only at t_1. On the other hand, $\mathbf{x}_{DE}$ is continuous and relaxes towards $\mathbf{c}_{DE}(t_1)$ during the time interval $[t_1, t_2)$ according to the formula

$$\mathbf{x}_{DE}(t) = \mathbf{c}_{DE}(t_1) + (\mathbf{x}_{DE}(t_1) - \mathbf{c}_{DE}(t_1))\exp\left(-\frac{(t-t_1)\sum_{i=1}^n \alpha_i \psi_i(t_1)}{\mu}\right). \tag{3}$$

Without loss of generality, we can assume that the attachment/detachment event at time t_1 involves I-site 1. It is convenient to consider 3 cases:

1. $\psi_1(t_1) = 0$ and $|\Psi(t_1)| = 0$;
2. $\psi_1(t_1) = 0$ and $|\Psi(t_1)| > 0$;
3. $\psi_1(t_1) = 1$.

In case 1 (the only attached I-site detaches),

$$(\mathbf{u}_Z(t), \mathbf{u}_{DE}(t), \mathbf{c}_Z(t), \mathbf{c}_{DE}(t), \mathbf{x}_Z(t)) = (\mathbf{u}_Z(t_1^-), \mathbf{u}_{DE}(t_1^-), \mathbf{c}_Z(t_1^-), \mathbf{c}_{DE}(t_1^-), \mathbf{x}_Z(t_1^-))$$

for every $t \in [t_1, t_2)$, so (3) gives

$$\mathbf{x}_{DE}(t) = \mathbf{c}_{DE}(t_1^-) + (\mathbf{x}_{DE}(t_1^-) - \mathbf{c}_{DE}(t_1^-)) \exp\left(-\frac{(t-t_1)\sum_{i=1}^n \alpha_i \psi_i(t_1)}{\mu}\right) = \mathbf{x}_{DE}(t_1^-).$$

Thus,

$$\|\mathbf{y}_{DE}(t_2^-) - \mathbf{y}_Z(t_2^-)\| = \|\mathbf{y}_{DE}(t_1^-) - \mathbf{y}_Z(t_1^-)\|.$$

Before proceeding to cases 2 and 3, we derive some estimates that hold in both cases. Let $t \in [t_1, t_2)$ and note that

$$\begin{aligned}
|\mathbf{c}_{DE}(t) - \mathbf{c}_Z(t)| &= \left|\sum_{i=1}^n \left(\frac{\alpha_i \psi_i(t)}{\sum_{j=1}^n \alpha_j \psi_j(t)}\right)(\mathbf{u}_{DE})_i(t) - \sum_{i=1}^n \left(\frac{\alpha_i \psi_i(t)}{\sum_{j=1}^n \alpha_j \psi_j(t)}\right)(\mathbf{u}_Z)_i(t)\right| \\
&\le \sum_{i=1}^n \left(\frac{\alpha_i \psi_i(t)}{\sum_{j=1}^n \alpha_j \psi_j(t)}\right)|(\mathbf{u}_{DE})_i(t_1) - (\mathbf{u}_Z)_i(t_1)| \\
&\le \sum_{i=1}^n \left(\frac{\alpha_i \psi_i(t)}{\sum_{j=1}^n \alpha_j \psi_j(t)}\right)\max_j |(\mathbf{u}_{DE})_j(t_1) - (\mathbf{u}_Z)_j(t_1)| \\
&= \max_j |(\mathbf{u}_{DE})_j(t_1) - (\mathbf{u}_Z)_j(t_1)|. \qquad (4)
\end{aligned}$$

Similarly,

$$\begin{aligned}
|\mathbf{c}_{DE}(t_1)| &= \left|\sum_{i=1}^n \left(\frac{\alpha_i \psi_i(t_1)}{\sum_{j=1}^n \alpha_j \psi_j(t_1)}\right)(\mathbf{u}_{DE})_i(t_1)\right| \le \sum_{i=1}^n \left(\frac{\alpha_i \psi_i(t_1)}{\sum_{j=1}^n \alpha_j \psi_j(t_1)}\right)|(\mathbf{u}_{DE})_i(t_1)| \\
&\le \sum_{i=1}^n \left(\frac{\alpha_i \psi_i(t_1)}{\sum_{j=1}^n \alpha_j \psi_j(t_1)}\right)\max_j |(\mathbf{u}_{DE})_j(t_1)| = \max_j |(\mathbf{u}_{DE})_j(t_1)|. \qquad (5)
\end{aligned}$$

Using (3), (4), and (5), we have

$$\begin{aligned}
|\mathbf{x}_{DE}(t_2^-) - \mathbf{x}_Z(t_2^-)| &= \Big|\mathbf{c}_{DE}(t_1) + (\mathbf{x}_{DE}(t_1) - \mathbf{c}_{DE}(t_1)) \exp\left(-\frac{(t_2-t_1)\sum_{i=1}^n \alpha_i \psi_i(t_1)}{\mu}\right) \\
&\quad - \mathbf{x}_Z(t_2^-)\Big| \\
&\le |\mathbf{c}_{DE}(t_1) - \mathbf{x}_Z(t_2^-)| + (|\mathbf{x}_{DE}(t_1)| + |\mathbf{c}_{DE}(t_1)|) \exp\left(-\frac{(t_2-t_1)\sum_{i=1}^n \alpha_i \psi_i(t_1)}{\mu}\right) \\
&\le |\mathbf{c}_{DE}(t_1) - \mathbf{c}_Z(t_1)| + (|\mathbf{x}_{DE}(t_1^-)| + |\mathbf{c}_{DE}(t_1)|) \exp\left(-\frac{(t_2-t_1)\min_i \alpha_i}{\mu}\right) \\
&\le \max_j |(\mathbf{u}_{DE})_j(t_1) - (\mathbf{u}_Z)_j(t_1)| \\
&\quad + (M + \max_j |(\mathbf{u}_{DE})_j(t_1)|) \exp\left(-\frac{(t_2-t_1)\min_i \alpha_i}{\mu}\right). \qquad (6)
\end{aligned}$$

Now, consider case 2 specifically (an attached I-site detaches leaving other attached sites). Here, $(\mathbf{u}_Z(t), \mathbf{u}_{DE}(t)) = (\mathbf{u}_Z(t_1^-), \mathbf{u}_{DE}(t_1^-))$ for every $t \in [t_1, t_2)$, so

$$|(\mathbf{u}_{DE})_i(t_2^-) - (\mathbf{u}_Z)_i(t_2^-)| = |(\mathbf{u}_{DE})_i(t_1) - (\mathbf{u}_Z)_i(t_1)| = |(\mathbf{u}_{DE})_i(t_1^-) - (\mathbf{u}_Z)_i(t_1^-)|, \tag{7}$$

for every i, and combining (4) with (7) gives

$$|\mathbf{c}_{DE}(t_2^-) - \mathbf{c}_Z(t_2^-)| \leq \|\mathbf{y}_{DE}(t_1^-) - \mathbf{y}_Z(t_1^-)\|. \tag{8}$$

Combining (6) with (7) and the fact that $\max_j |(\mathbf{u}_{DE})_j(t_1)| = \max_j |(\mathbf{u}_{DE})_j(t_1^-)| \leq M$ gives

$$|\mathbf{x}_{DE}(t_2^-) - \mathbf{x}_Z(t_2^-)| \leq \|\mathbf{y}_{DE}(t_1^-) - \mathbf{y}_Z(t_1^-)\| + 2M \exp\left(-\frac{(t_2 - t_1)\min_i \alpha_i}{\mu}\right). \tag{9}$$

Using (7), (8), and (9), we have

$$\|\mathbf{y}_{DE}(t_2^-) - \mathbf{y}_Z(t_2^-)\| \leq \|\mathbf{y}_{DE}(t_1^-) - \mathbf{y}_Z(t_1^-)\| + 2M \exp\left(-\frac{(t_2 - t_1)\min_i \alpha_i}{\mu}\right).$$

Finally, consider case 3 specifically (a detached I-site attaches), and let $t \in [t_1, t_2)$. Here,

$$((\mathbf{u}_Z)_1(t), (\mathbf{u}_{DE})_1(t)) = (\mathbf{c}_Z(t_1^-) + \mathbf{b}^{p,1}, \mathbf{x}_{DE}(t_1^-) + \mathbf{b}^{p,1})$$

for some $\mathbf{b}^{p,1} \in \mathbb{R}^N$ satisfying $|\mathbf{b}^{p,1}| \leq B$, while

$$((\mathbf{u}_Z)_i(t), (\mathbf{u}_{DE})_i(t)) = ((\mathbf{u}_Z)_i(t_1^-), (\mathbf{u}_{DE})_i(t_1^-))$$

for every $i \neq 1$ a.s. Thus,

$$\begin{aligned} |(\mathbf{u}_{DE})_i(t_2^-) - (\mathbf{u}_Z)_i(t_2^-)| &= \begin{cases} |(\mathbf{u}_{DE})_i(t_1^-) - (\mathbf{u}_Z)_i(t_1^-)| & \text{if } i \neq 1 \\ |\mathbf{x}_{DE}(t_1^-) - \mathbf{c}_Z(t_1^-)| & \text{if } i = 1 \end{cases} \\ &\leq \|\mathbf{y}_{DE}(t_1^-) - \mathbf{y}_Z(t_1^-)\|. \end{aligned} \tag{10}$$

Combining (4) with (10) gives

$$|\mathbf{c}_{DE}(t_2^-) - \mathbf{c}_Z(t_2^-)| \leq \|\mathbf{y}_{DE}(t_1^-) - \mathbf{y}_Z(t_1^-)\|. \tag{11}$$

Combining (6) with (10) and the fact that

$$\max_j |(\mathbf{u}_{DE})_j(t_1)| \leq \max\{\max_{j \neq 1} |(\mathbf{u}_{DE})_j(t_1^-)|, |\mathbf{x}_{DE}(t_1^-)| + |\mathbf{b}^{p,1}|\} \leq M + B$$

gives

$$|\mathbf{x}_{DE}(t_2^-) - \mathbf{x}_Z(t_2^-)| \leq \|\mathbf{y}_{DE}(t_1^-) - \mathbf{y}_Z(t_1^-)\| + (2M + B) \exp\left(-\frac{(t_2 - t_1)\min_i \alpha_i}{\mu}\right). \tag{12}$$

Using (10), (11), and (12), we have

$$\|\mathbf{y}_{DE}(t_2^-) - \mathbf{y}_Z(t_2^-)\| \leq \|\mathbf{y}_{DE}(t_1^-) - \mathbf{y}_Z(t_1^-)\| + (2M + B)\exp\left(-\frac{(t_2 - t_1)\min_i \alpha_i}{\mu}\right).$$

Combining the results of all 3 cases, we see that

$$\|\mathbf{y}_{DE}(t_2^-) - \mathbf{y}_Z(t_2^-)\| \leq \|\mathbf{y}_{DE}(t_1^-) - \mathbf{y}_Z(t_1^-)\| + (2M + B)\exp\left(-\frac{(t_2 - t_1)\min_i \alpha_i}{\mu}\right)$$

holds a.s. □

The second lemma bounds the norm of the state variables after k attachment/detachment events in terms of the initial state and properties of the distribution η.

Lemma 4.3. *Assume that $k \geq 1$ attachment/detachment events occur at times $0 < t_1 < t_2 < \cdots < t_k$ in the interval $[0, t)$ and no other attachment/detachment events occur. Define*

$$M_i := \|\mathbf{y}_{DE}(t_i^-)\| \text{ for } i = 1, \ldots, k$$

and let B be such that $\eta(\mathcal{B}(0, B)) = 1$. Then

$$M_i \leq M_1 + (i - 1)B \quad \text{a.s.}$$

Proof. First we find bounds on the location of the cell center $\mathbf{x}$. From (3) the location of the cell center for $t \in [t_i, t_{i+1})$ is

$$\begin{aligned}\mathbf{x}_{DE}(t) &= \mathbf{c}_{DE}(t_i) \\ &\quad + (\mathbf{x}_{DE}(t_i) - \mathbf{c}_{DE}(t_i))\exp\left(-\frac{(t - t_i)\sum_{j=1}^n \alpha\psi_j(t_i)}{\mu}\right).\end{aligned}$$

Since

$$\begin{aligned}|\mathbf{c}_{DE}(t_i) - \mathbf{x}_{DE}(t_i)| &= \left|\frac{\sum_{j=1}^n \alpha_j[(\mathbf{u}_{DE})_j(t_i) - \mathbf{x}_{DE}(t_i)]\psi_j(t_i)}{\sum_{j=1}^n \alpha_j\psi_j(t_i)}\right| \\ &= \left|\frac{\sum_{j=1}^n \alpha_j \mathbf{b}^{i,j}\psi_j(t_i)}{\sum_{j=1}^n \alpha_j\psi_j(t_i)}\right| \\ &< B\end{aligned}$$

a.s., $\mathbf{x}_{DE}$ can be bounded by

$$|\mathbf{x}_{DE}(t)| \leq |\mathbf{c}_{DE}(t_i) - \mathbf{x}_{DE}(t_i)| + |\mathbf{c}_{DE}(t_i)| \leq B + M_i. \tag{13}$$

Next we find bounds on the location of the centroid. Using the bound just found in (13),

$$\begin{aligned}|\mathbf{c}_{DE}(t_i)| &= \left|\frac{\sum_{j=1}^n \alpha_j (\mathbf{u}_{DE})_j(t_i)\psi_j(t_i)}{\sum_{j=1}^n \alpha_j \psi_j(t_{i+1})}\right| \\ &= \left|\frac{\sum_{j=1}^n \alpha_j (\mathbf{x}_{DE}(t_i) + \mathbf{b}^{i,j})\psi_j(t_i)}{\sum_{j=1}^n \alpha_j \psi_j(t_i)}\right| \\ &\leq |\mathbf{x}_{DE}(t_i)| + \max_j |\mathbf{b}^{i+1,j}| < B + M_i.\end{aligned}$$

Finally we bound the location of the I-sites in the same manner as above,

$$\begin{aligned}|(\mathbf{u}_{DE})_j(t_i)| &= |\mathbf{x}_{DE}(t_i) + \mathbf{b}^{i,j}| \\ &\leq |\mathbf{x}_{DE}(t_i)| + |\mathbf{b}^{i,j}| < B + M_i\end{aligned}$$

Thus we have

$$M_{i+1} = \|\mathbf{y}(t_{i+1}^-)\| < B + M_i \quad \text{a.s.} \quad \square$$

4.3. *Proof of EVR theorem*

With a bound on the "distance" between the centroid model and the differential equation model between attach/detach events, we can consider a time interval partitioned by some finite number of events to prove the EVR Theorem.

Proof. Lemma 4.2 gives a.s.

$$\|\mathbf{y}_{DE}(t^-) - \mathbf{y}_Z(t^-)\| \leq \|\mathbf{y}_{DE}(s^-) - \mathbf{y}_Z(s^-)\| + (2\|\mathbf{y}_{DE}(s^-)\| + B)e^{-C(t-s)} \tag{14}$$

if an attachment/detachment event occurs at time $s < t$, and no such events occur on the interval (s, t), where B bounds the support of the perturbation distribution η, and $C = \alpha/\mu$ is a measure of the spring strength that will eventually be sent to ∞. The quantities $\mathbf{y}_{DE}$ and $\mathbf{y}_Z$ are random, but (14) holds along each sample path.

We can choose the initial state of the centroid model, so we let $\mathbf{y}_{DE}(0) = \mathbf{y}_Z(0)$. Recall that $\mathbf{x}_{DE}(0) = \mathbf{x}_Z(0)$ since $\mathbf{x}_{DE}(0)$ is at equilibrium position. From [1] we know the value of $\mathbb{E}[\mathbf{x}_Z(t) - \mathbf{x}_Z(0)] = \mathbb{E}[\mathbf{c}_Z(t) - \mathbf{c}_Z(0)]$ in terms of θ_a, θ_d, and $\overline{\mathbf{b}}$ (under reasonable restrictions on the initial data). We want to show that

$$\lim_{C\to\infty} \mathbb{E}[\mathbf{x}_{DE}(t) - \mathbf{x}_{DE}(0)] = \mathbb{E}[\mathbf{x}_Z(t) - \mathbf{x}_Z(0)]. \tag{15}$$

Consider

$$\mathbb{E}[\mathbf{x}_{DE}(t) - \mathbf{x}_{DE}(0)] = \mathbb{E}[\mathbf{x}_{DE}(t) - \mathbf{x}_Z(t) + \mathbf{x}_Z(t) - \mathbf{x}_Z(0) + \mathbf{x}_Z(0) - \mathbf{x}_{DE}(0)].$$

Regrouping terms we have

$$\mathbb{E}[\mathbf{x}_{DE}(t) - \mathbf{x}_{DE}(0)] = \mathbb{E}[\mathbf{x}_{DE}(t) - \mathbf{x}_Z(t)] + \mathbb{E}[\mathbf{x}_Z(0) - \mathbf{x}_{DE}(0)] + \mathbb{E}[\mathbf{x}_Z(t) - \mathbf{x}_Z(0)].$$

Due to the hypotheses, the middle term is zero and if

$$\lim_{C\to\infty} \mathbb{E}[\mathbf{x}_{DE}(t) - \mathbf{x}_Z(t)] = 0, \tag{16}$$

then (15) is valid. By (2) we would then have the desired result

$$\lim_{C\to\infty} \mathbb{E}[\mathbf{x}(t)] - \mathbb{E}[\mathbf{x}(0)] = \frac{\overline{\boldsymbol{b}}\theta_d}{(\theta_d+\theta_a)^n}\left((\theta_d+\theta_a)^n - \theta_d^n\right)t.$$

In order to show (16) it suffices to show that the differential equation model and the centroid model, when starting at the same state, in the limit evolve to the same state; that is to say

$$\lim_{C\to\infty} \mathbb{E}\|\mathbf{y}_{DE}(t) - \mathbf{y}_Z(t)\| = 0. \tag{17}$$

We show this using the Dominated Convergence Theorem and the results of Lemmas 4.2 and 4.3.

Let $f(C,\omega) := \|\mathbf{y}_{DE}(t) - \mathbf{y}_Z(t)\|$. For each nonnegative integer i, let A_i be the event that there are precisely i attachments and detachments in the time interval from 0 to t, and let A_∞ be the complement of $A_0 \cup A_1 \cup A_2 \cup \cdots$.

We will show that $\mathbb{P}(A_\infty) = 0$, that $\lim_{C\to\infty} f(C,\omega) = 0$ for each $\omega \notin A_\infty$, and that there is an integrable function g of ω alone such that $f(C,\omega) \le g(\omega)$ for every $\omega \notin A_\infty$. The Dominated Convergence Theorem will then establish (17).

The event A_i is the event that i attachment/detachments occur in the time interval $[0,t]$. The time between the $(k-1)$th and kth attachment/detachments is of the form γ_k/Θ_k, where the γ_k are independent standard exponential random variables and the Θ_k are random variables that are bounded above by $D_I := n\max\{\theta_a,\theta_d\}$. If the event A_i is realized, then

$$t \ge \sum_{k=1}^{i} \gamma_k/\Theta_k \ge \frac{\sum_{k=1}^{i}\gamma_k}{D_I},$$

so $E_i := \sum_{k=1}^{i}\gamma_k \le D_I t$. But E_i is Erlang-distributed with shape parameter i and rate parameter 1, which means that its distribution function is $x \mapsto e^{-x}\sum_{k=i}^{\infty}(x^k/k!)$ [5]. If more than i events occur in the time interval, the same inequality holds. Thus,

$$\mathbb{P}(A_\infty \cup \bigcup_{k=i}^{\infty} A_k) \le \exp(-D_I t)\sum_{k=i}^{\infty}\frac{(D_I t)^k}{k!}.$$

By the Ratio Test and the Divergence Test, this gives $\mathbb{P}(A_\infty) = 0$.

For $\omega \in A_0$, no events happen and all variables of the ODE model and the centroid model stay at the same place, since they started at the same state and $\mathbf{x}_{DE}$ is at equilibrium. Thus $f(C,\omega) = 0$. For $\omega \in A_k$ where $k \ge 1$, k events occur in the interval $[0,t]$. Thus k events occur in the open interval $(0,t)$ a.s. since the wait times are exponentially distributed. Let $0 < t_1 < t_2 < \cdots < t_k$, be the times that the events occur, $t_0 = 0$, and $t_{k+1} = t$. Since no events occur a.s. at t, $f(C,\omega) = \|\mathbf{y}_{DE}(t^-) - \mathbf{y}_Z(t^-)\|$, and applying Lemma 4.2

$$\begin{aligned}\|\mathbf{y}_{DE}(t^-) - \mathbf{y}_Z(t^-)\| &= \|(\mathbf{y}_{DE}(t_{k+1}^-) - \mathbf{y}_Z(t_{k+1}^-))\| \\ &\leq \|\mathbf{y}_{DE}(t_k^-) - \mathbf{y}_Z(t_k^-)\| + (2M_k + B)\exp\left(-(t_{k+1} - t_k)C\right).\end{aligned}$$

Applying Lemma 4.2 recursively gives

$$\|\mathbf{y}_{DE}(t_{k+1}^-) - \mathbf{y}_Z(t_{k+1}^-)\| \leq \sum_{j=1}^{k}(2M_j + B)\exp\left(-(t_{j+1} - t_j)C\right)$$

where $M_j = \|\mathbf{y}_{DE}(t_j^-)\|$. Let $T(\omega) = \min_j(t_j - t_{j-1})$ and the above equations give

$$\|\mathbf{y}_{DE}(t_{k+1}^-) - \mathbf{y}_Z(t_{k+1}^-)\| \leq \sum_{j=1}^{k}(2M_j + B)\exp\left(-T(\omega)C\right).$$

Applying Lemma 4.3 gives for $k \geq 2$,

$$\|\mathbf{y}_{DE}(t_{k+1}^-) - \mathbf{y}_Z(t_{k+1}^-)\| \leq 2k\left\{B(k+1) + M_1\right\}\exp\left(-T(\omega)C\right).$$

So for a fixed $k \geq 0$, $f(C,\omega) \leq 2(B(k+1) + M_1)k$ a.s. for $\omega \in A_k$. Furthermore $\lim_{C\to\infty} f(C,\omega) = 0$ a.s.

Finally let $g(\omega) = \sum_{k=0}^{\infty} 2(B(k+1) + M_1)k\mathbb{1}_{A_k(\omega)} \geq 0$.

$$\mathbb{E}[g] \leq \sum_{k=0}^{\infty} 2(B(k+1) + M_1)k\exp(-D_I t)\sum_{j=k}^{\infty}\frac{(D_I t)^j}{j!}.$$

Stirling's formula gives $j! \geq \sqrt{2\pi}\, j^{j+\frac{1}{2}}\exp(-j) \geq j^{j+\frac{1}{2}}\exp(-j)$. Thus

$$\sum_{j=k}^{\infty}\frac{(D_I t)^j}{j!} \leq \sum_{j=k}^{\infty}\frac{(eD_I t)^j}{j^{j+\frac{1}{2}}} \leq \sum_{j=k}^{\infty}\left(\frac{eD_I t}{j}\right)^j.$$

Thus

$$\mathbb{E}[g] \leq \sum_{k=0}^{\infty} 2(B(k+1) + M_1)k\exp(-D_I t)\sum_{j=k}^{\infty}\left(\frac{eD_I t}{j}\right)^j. \tag{18}$$

For $k \geq 4eD_I t$, we have

$$\sum_{j=k}^{\infty}\frac{(D_I t)^j}{j!} \leq \sum_{j=k}^{\infty}\left(\frac{eD_I t}{j}\right)^j \leq \sum_{j=k}^{\infty}\left(\frac{1}{4}\right)^j = \sum_{j=0}^{\infty}\left(\frac{1}{4}\right)^{j+k} = \frac{4}{3}\left(\frac{1}{4}\right)^k.$$

Applying the ratio test to the series in (18) shows that $\mathbb{E}[g] < \infty$. The conditions for the Dominated Convergence Theorem are met and ((17)) is valid. □

Due to the time invariance of the processes and distributions, the time interval $[0, t]$ can be translated without affecting the results. This is stated in the following corollary

Corollary 4.4. *Assume the configuration at time t_0 for (1) is randomly distributed in a way that is compatible with the steady-state distribution σ. Moreover assume $\alpha_i = \alpha$ for all i and that $\mathbf{x}_{DE}(t_0) = \mathbf{x}_Z(t_0)$. For a fixed time $t > t_0$,*

$$\lim_{\frac{\alpha}{\mu}\to\infty} \mathbb{E}[\mathbf{x}(t + t_0)] - \mathbb{E}[\mathbf{x}(t_0)] = \boldsymbol{\zeta} t.$$

In the case where $\mathbf{x}(0)$ is not an equilibrium, the following corollary applies.

Corollary 4.5. *Let $\mathbf{d_0} = \mathbf{x}_{DE}(0) - \mathbf{x}_Z(0)$. Then*

$$\lim_{\frac{\alpha}{\mu}\to\infty} \|\mathbb{E}[\mathbf{x}(t) - \mathbf{x}(0)]\| \leq 2\|\mathbf{d_0}\| + \|\boldsymbol{\zeta}\| t.$$

Proof. By a simple modification of the proof of the EVR theorem,

$$\begin{aligned}\mathbb{E}[\mathbf{x}_{DE}(t) - \mathbf{x}_{DE}(0)] &= \mathbb{E}[\mathbf{x}_{DE}(t) - \mathbf{x}_Z(t)] + \mathbb{E}[\mathbf{x}_Z(t) - \mathbf{x}_Z(0)] + \mathbb{E}[\mathbf{x}_Z(0) - \mathbf{x}_{DE}(0)] \\ &= \mathbb{E}[\mathbf{x}_{DE}(t) - \mathbf{x}_Z(t)] + \boldsymbol{\zeta} t + \mathbf{d_0}.\end{aligned}$$

Taking the norm of both sides

$$\begin{aligned}\|\mathbb{E}[\mathbf{x}_{DE}(t) - \mathbf{x}_{DE}(0)]\| &= \|\mathbb{E}[\mathbf{x}_{DE}(t) - \mathbf{x}_Z(t)] + \boldsymbol{\zeta} t + \mathbf{d_0}\| \\ &\leq \mathbb{E}[\|\mathbf{x}_{DE}(t) - \mathbf{x}_Z(t)\|] + \|\boldsymbol{\zeta}\| t + \|\mathbf{d_0}\|.\end{aligned}$$

The function in the expectation is dominated by $g(\omega) + \|\mathbf{d_0}\|$. Taking the limit as $\frac{\alpha}{\mu} \to \infty$ gives the result. □

5. Numerical results

Numerical simulations confirm the theoretical results and suggest a different result for non-Markov processes. The differential equation is solved using the software CVODE [11], in one second intervals. If an attachment event is due or past due, the differential equation with the new state is solved. Fig. 3 shows 5 realizations where the cell is starting at $(0, 0)$. The distribution for the perturbation vector $\mathbf{b}$ is isotropic, so on average there should be no motion. The vector $\mathbf{b}$ is chosen by randomly choosing an angle from a uniform distribution and a radius from a uniform distribution. Wait times are also chosen from a specified distribution.

Fig. 4 shows a graph of the equation for ζ from the EVR theorem in both panels and in the left panel simulation results where different values for $\frac{\alpha}{\mu}$ are used and in the right panel simulation results with different wait time distributions are shown. In the left panel one can see the convergence to the theoretical results. In the right panel the exponential wait times fit fairly well with the theory, although the simulation results are consistently slower than the theoretical results for more I-sites. This is expected since the differential equation has a viscous drag which should slow the cells down. (The drag contribution disappears only in the limit. Thus in the left

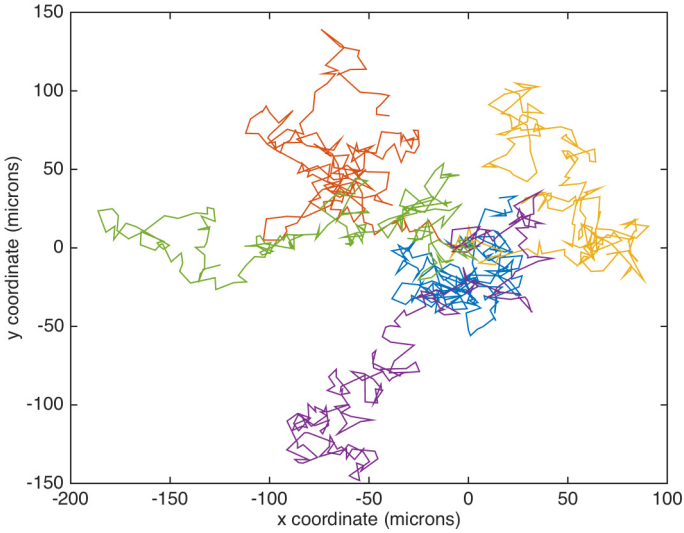

Fig. 3. Five realizations for cells are shown for simulations of about 35 hours. The random perturbations **b** are isotropic with mean radius 2.5 microns. The wait distributions are exponential with $\theta_d = \frac{1}{20s}$, $\theta_a = \frac{1}{60s}$, $\alpha_i = 0.2$ nN/micron for all i, $i = 30$, and $\mu = 2.8 \times 10^{-7}$ kg/s. The initial configuration for each realization was created by running a simulation which started with all I-sites attached for at least 1000 hours and translating the resulting position to the origin. Thus the projection of the initial state (starting from the 1000 hours) should be converging to the steady state distribution assumed in the EVR theorem. The cell location is plotted every 10 minutes.

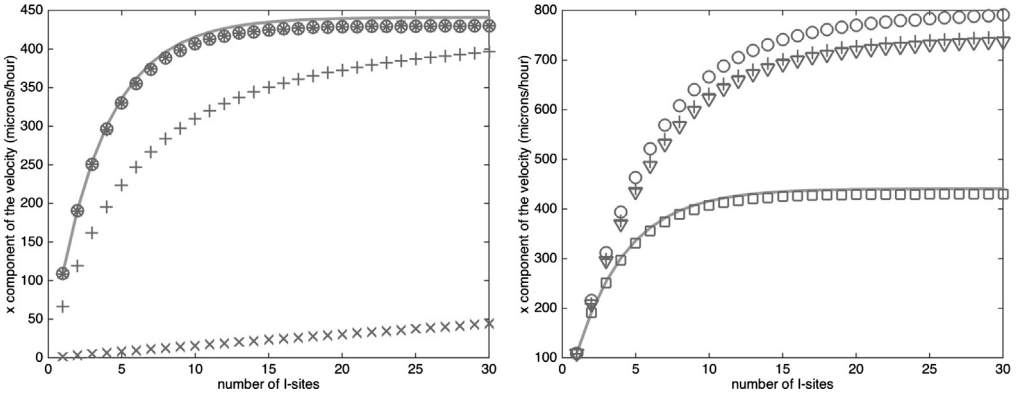

Fig. 4. Simulations showing the convergence to the theoretical result are shown in the left panel and simulations with different wait time distributions are shown on the right. The time derivative of the expected value of the x coordinate of the cell center is plotted in microns per hour against the number of I-sites. In both panels the gray line shows ζ as given in the EVR theorem. In the left panel expected velocity of simulations are shown with $\frac{\alpha}{\mu} = 740$, 7.4, .074, and 7.4×10^{-4} in units of 1/seconds with circles, *, +, and $\times$ respectively. In the right panel simulations with wait time drawn from exponential, normal, continuous Poisson, and uniform distributions are shown by boxes, circles, +, and $\triangledown$ respectively. The simulations were run for 3,333 hours to avoid error due to initial conditions and then the average velocity was taken over a time period of 6,666 hours. Due to the time homogeneity this is the same as averaging many simulations. The mean time to detachment is 60 seconds and the mean time to attachment is 20 seconds for all the simulations. The normal distributions had deviation of 1 second (and were truncated to prevent negative and very long positive times). The random vector **b** has a propensity to be in the x direction.

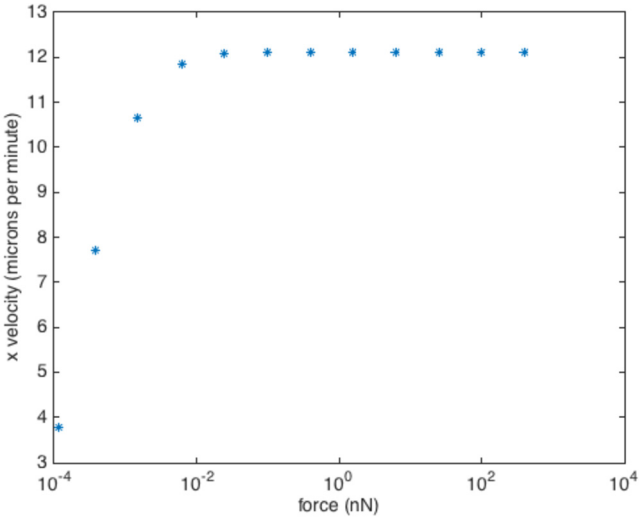

Fig. 5. The average x coordinate of the velocity is plotted against the average force the cell exerts on the substrate. Each data point is the average of 30 simulations with the same spring constant α. The spring constant was varied from $2.0 \times 10^{-7} - 0.3$ nN/micron. Notice the scale on the x axis is logarithmic. Realistic forces for cells range from 0.1-2000 nN all forces where the velocity has already reached a constant value for these simulations. For each simulation the number of sites is fixed at 20. The other parameters are the same as the previous figure with the continuous Poisson distribution. Each simulation was run for 100 hours and then data was collected for the next 200 hours.

panel the lower values of $\frac{\alpha}{\mu}$ are slower than the theoretical results.) The other non-Markovian distributions indicate that the Markov property is essential in our current work. In Fig. 5, the x coordinate of the velocity is plotted against the force. As can be readily seen in the figure the velocity is asymptotically constant with respect to the cell force. Realistic forces range from 0.1 nN to thousands of nanoNewtons which is in the region where the velocity is almost constant. These simulations used a continuous Poisson distribution for the wait times and thus do not fit into the framework of the theory given in this paper. Yet the qualitative result is similar for the exponential wait times, that is, the velocity quickly approaches a constant value at forces much lower than experimentally measured values.

Finally, in Fig. 6 we compare experimental data of cell motion vs the model cell motion taken from [4]. Results from simulations of the differential equation model (1) are used to calculate average cell speed for a range of cell strengths and a range of mean attach times. The mean detach time is fixed and the cell forces for each I-site are set to be the same, i.e. $\alpha = \alpha_i$ for all i. The model cells exhibit speeds and forces which agree with experimental data. The range of values for α and for the mean attach time respectively are 0.232-4.44 nN/micron and 810-1210 seconds for fibroblasts, 1.17-2.33 nN/micron and 28-88 seconds for neutrophils, 0.233-0.614 nN/micron and 230-408 seconds for murine dendritic cells, 1.17-1.18 nN/micron and 206-408 for endothelial cells, and 0.116-0.348 nN/micron and 18-70 seconds for Dd cells.

6. Discussion

The models discussed in this paper represent part of a broader approach to cell motion dynamics, advancing the application of probabilistic arguments outside the common core of treatments (Brownian motion) for stochastic media [8]. In cell migration, it has been known for some time

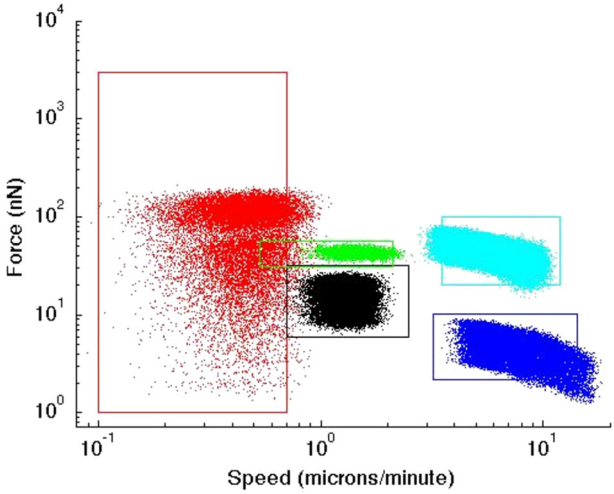

Fig. 6. The boxes roughly outline the regions where experimental data has been reported for different cells types. The scatter plots are simulation results with parameters used to mimic the behavior of the different cells using the differential equation model. Red denotes fibroblasts, black denotes murine dendritic cells, cyan denotes neutrophils, green denotes endothelial cells, and blue denotes Dd cells. Figure taken from [4] with permission. (For interpretation of the colors in the figure(s), the reader is referred to the web version of this article.)

that higher cell force does not correlate in an obvious way with cell velocity. The models analyzed here encode this fact in several ways. Our previous work suggested that cell adhesion/binding behavior was at the heart of the problem of modeling cell velocity. Cell strength (force exerted on a substrate) impacts mechanosensing properties of the cell, but is less important in cell velocity [4]. Numerical simulations in [4] led to our conjecture of the EVR, which symbolically models the decoupling of cell strength and velocity by considering average cell velocity over a fixed time interval, as cell strength increases relative to drag force. In [2], we introduced a limit version of the differential equation model (a discrete-time centroid model) of [4], and analyzed this centroid model and the EVR using Markov chain theory. A heuristic argument in [2] reinforced the idea that the EVR conjecture holds in the case of the original random differential equation model. There, the decoupling of force and speed is suggested by the centroid model showing that new adhesion sites cause the cell to shift quickly after a cell attachment/detachment event (even though between shifts, substrate tension remains high). We formalized the relationship between a centroid model and the differential equation model by studying the problem in the framework of dynamical systems, first by passing to an intermediate continuous-time centroid model [1]. The mathematical formalization of the models allows for a rigorous treatment of the EVR conjecture in the differential equation model using our previous work for the discrete models. The present work breaks ground in the rigorous study of randomly switched differential equations with the proof of the EVR conjecture in Theorem 4.1.

This work provides a rigorous modeling environment for cell motion at the macro level (it does not treat the internal biophysical mechanisms in an individual cell). We plan to investigate non-Markov scenarios in future work. Future work also promises the possibility of rigorously linking microcellular processes with macrocellular motion. Moreover, the differential equation model may be shown to provide insight into multicellular environments. Future work will demonstrate this and provide effective modeling of important macro-cellular processes like cancer metastases,

conglomerate cell motion (for example, Dictyostelium discoideum [3]) and other types of cell migration. Additionally, this model could have applications in the motion of swarms and schools including crowd behavior, aggregate cell motion, and certain types of neural nets. All these systems have centrally organized motion which could fit into our model framework. Man-made centrally controlled or centrally referenced motion occurs in monetary markets, the movement of troops or equipment on the battlefield, and the evolution of social networks. These applications will be investigated in future work.

References

[1] J.C. Dallon, L.C. Despain, E.J. Evans, C.P. Grant, W.V. Smith, A continuous-time model of centrally coordinated motion with random switching, J. Math. Biol. (2016) 1–27.
[2] J.C. Dallon, E.J. Evans, C.P. Grant, W.V. Smith, Cell speed is independent of force in a mathematical model of amoeboidal cell motion with random switching terms, Math. Biosci. 246 (2013) 1–7.
[3] J.C. Dallon, H.G. Othmer, How cellular movement determines the collective force generated by the *Dictyostelium discoideum* slug, J. Theor. Biol. 231 (2004) 203–222.
[4] J.C. Dallon, M. Scott, W.V. Smith, A force based model of individual cell migration with discrete attachment sites and random switching terms, J. Biomech. Eng. 135 (2013) 071008.
[5] C. Forbes, M. Evans, N. Hastings, B. Peacock, Erlang Distribution, John Wiley & Sons, Inc., 2010, pp. 84–85.
[6] P. Friedl, D. Gilmour, Collective cell migration in morphogenesis, regeneration and cancer, Nat. Rev. Mol. Cell Biol. 10 (2009) 445–457.
[7] B.M. Gumbiner, Cell adhesion: the molecular basis of tissue architecture and morphogenesis, Cell 84 (1996) 345–357.
[8] E.L. Ionides, K.S. Fang, R.R. Isseroff, G.F. Oster, Stochastic models for cell motion and taxis, J. Math. Biol. 48 (2004) 23–37.
[9] G. Marsaglia, The incomplete γ function as a continuous Poisson distribution, Comput. Math. Appl. 12 (1986) 1187–1190.
[10] F. Ulrich, C.-P. Heisenberg, Trafficking and cell migration, Traffic 10 (2009) 811–818.
[11] C. Woodward, A.C. Hindmarsh, R. Serban, SUNDIALS (Suite of Nonlinear and DIfferential/ALgebraic Equation Solvers), Copyright © 2002, The Regents of the University of California, 2012, Produced at the Lawrence Livermore National Laboratory.